Stochastic Modeling and Applications
Vol. 25 No. 2 (July-December, 2021)
ISSN: 0972-3641

Received: 17th December 2021 Revised: 29th December 2021 Selected: 31st December 2021

EFFECTS OF VARIABLE VISCOSITY AND THERMAL CONDUCTIVITY ON MHD FLOW DUE TO THE PERMEABLE MOVING PLATE

HIMANSHU CHAUDHARY[1*], DEENA SUNIL[2], VISHNU NARAYAN MISHRA[3]

Abstract- *This work address the impacts of thermo-physical properties on convective heat transfer of Magneto hydrodynamics slip flow due to permeable moving plate. The governing heat and mass transfer nonlinear partial differential equations of fluid flow transformed into a system of nonlinear ordinary differential equations with the help of suitable similarity transformations. The Runge-Kutta 4th order with shooting technique are used to solve governing boundary value problems. Impact of prominent physical parameters like magnetic* (M)*, prandtl number* (Pr)*, eckert number* (Ec)*, schmidt number* (Sc)*, variable viscosity* (θ_r)*, thermal conductivity* (ε)*, surface convection* (a)*, velocity ratio* (λ) *and radiation* (Nr) *along their various values for velocity, temperature ,and concentration profile are represented as graphically and numerically. It is observed that the variable thermal conductivity and viscosity are the most prominent parameters responsible for different results of velocity, temperature and concentration.*

Keywords- *Boundary layer, Convective heat transfer, Moving plate, Slip flow.*

Introduction

Boundary layer flow across a flat plate in a uniform stream of fluid has grown more relevant due to its huge number of applications, including cooling nuclear reactors, polymer extrusion from a die, cooling of metallic sheets inside cooling bath, crystal formation, and heat transmission. It has numerous applications in the automobile industry, as well as in energy, such as boilers and home appliances. Presence of fluidconducting electrically, withthe occurrence of a magnetic field causes a resistance force that acts perpendicular to the magnetic field's direction. Many researchers have noticed Lorentz Magneto Hydrodynamics (MHD) drag, which delays flow within the thickening of the concentration boundary layer.

MHD is a concept of dealing between electrically conducting fluid and electromagnetic forces. Its effect occurs in so many natural phenomena, including the generation of the magnetic field of planets and stars, the Earth's magnetic field with solar wind as well as lightning. So many researchers encountered with MHD problems previously and it has many applications in sensors, engineering, geophysics, earthquakes and astrophysics etc [1].The magnetic field causes the boundary layer to thin, increasing wall friction, and this impact is stronger for shear thinning in compare to shear-thickening fluids [2].A transition value βc is a decreasing function of aspect ratio that divided the region of heat transfer enhancement and reduction [3]. It is noticed that the concentration buoyancy effects are increased with the rise in solutal Grash of number, and therefore, the fluid velocity also rises. The existence of heat absorption effects causes a decrease in fluid velocity as a result of decay in fluid temperature, and concentration level decreased as Sc grew.

Existence of slip conditions also affects the heat transfer process [4]. In liquid flows, heat transfer increases with respect to an increment in slip velocity where no temperature jump takes place. In the case of the flow of gases, however, a temperature difference is introduced, and the velocity slip is shown to scale with it. The heat transfer condition in the system decline in the occurrence of the thermal jump [5] noticed that with the decreasing of chemical reaction parameter all profiles the rises. The absorption parameterinfluence on velocity and temperature profile is alike [6] As power-law index n and Chandrasekhar number rises corresponding hydrodynamic boundary layer thickness reduces.If the convective heat transfer caused by the hot fluid on the plate's lower surface is proportional to $x^{\frac{-1}{2}}$, a similarity solution is possible studied by [7,8] gets the interfacial slip boundary conditions are also very effective for transfer in the respective boundary layer. For liquid slip flows, as a result of momentum slip, the no–slip value is less than heat transfer augmented[9] noticed that on heat transmission, the impacts of unsteadiness, suction/injection parameter, $Pr$are systematically investigated [10]. The mass suction and magnetic parameter is an increasing function of β.

The thermal conductivity enhancement promote higher velocities and temperature into the corresponding boundary layers[11] Whereas, as thermal conductivity increased, the wall shear stress increased [12].The magnitude of heat transfer and shear stress rate are similar to variations in A ,but M and R_d follows opposite behavior with local nusselt number [13].The liquids with high Prandtlby means of a low-slip coefficient, the heat transfer rate is high and a low magnetic parameter. In both circumstances, the Ec is significant in lowering the heat transmission rate and the viscous dissipation term is neglected for the high-slip coefficientinvestigated when there is no slip on the plate, the surface temperature is more and temperature of surface of the plate can be regulated in both slip and no-slip instances by varying the strength of the applied magnetic field[14].

Due to rise in M results to decreases fluid velocity slow in the presence of increasing magnetic parameter[15], due to effect of Lorentz force, which declining boundary layer thickness [16].At the interface of melt substrate heat and melting rate decreases with the increase in Lykoudis number. Over a melting substrate, a magnetic field is also utilised to calculate malting rate, free convection heat transfer, and boundary layers thickness of velocity and temperature.[17]. In the case of a stretched sheet, it has a single solution, however in the case of a shrinking sheet, numerous solutions were obtained when nanofluid was taken into account.The increases in viscous dissipation term, temperature rises, whereas it decreases with rise in radiation and suction [18].

With increasing Nb and Nt, the rate of heat transfer decreases.[19]. As Nt and Le are enhanced the Sherwood number also rises. But a decreasing function of Nb[20]. The concentration is decreasing function of the thermophoretic parameter[21].When the ε rises, the rate of heat transferand distribution of temperature at the wall drop. The Prandtl number holds thermal boundary layer. As Pr rises, so slow diffusion takes place; finally decline in the thermal boundary layer.

When variable viscosity increases, so does the flow and heat transfer. [22], but reverse tend followed in case of variable thermal conductivity that momentum slip enhances the velocity profile [23], but the impact is reverse for thermal and concentration profiles.

As per the above literature survey and our limited knowledge, due to permeable moving plate, there is no investigation available of different parameters like magnetic (M), prandtl number (Pr), eckert number (Ec), schmidt number (Sc), variable viscosity (θ_r), thermal conductivity (ε), surface convection (a), velocity ratio (λ) and radiation (Nr) with their diverse values for convective heat transfer of MHD slip flow problem. Hence, this paper aimed to discuss the effect of above-mentioned parameters on a permeable moving plate with their different values. The numerical and graphical result indicates that variable viscosity and thermal conductivity are the most noticeable parameters responsible for various results of velocity, temperature, and concentration of the considered problem.

MATHEMATICAL FORMULATION

In current study, a 2-D steady MHD laminar boundary layer flow problem with the heat and mass transfer over a flat plate and heat flux at boundary, with variable thermal conductivity and viscosity are considered. The B_0denotes theuniform magnetic field strengthwhich is applied perpendicular to the moving plate. Here $T_w$and T_∞ are wall and ambient temperature, respectively. Also, C_w is wall concentration and C_∞ is ambient concentration, respectively. In light of the above points, governing equations of heat and mass transfer are written by using boundary layer approximations:

$$\frac{\partial u}{\partial x}+\frac{\partial v}{\partial y}=0 \tag{1}$$

$$\rho\left(u\frac{\partial u}{\partial x}+v\frac{\partial u}{\partial y}\right)=\frac{\partial}{\partial y}\left(\mu\frac{\partial u}{\partial y}\right)-\sigma {B_0}^2(u-U_\infty) \tag{2}$$

$$\rho Cp\left(u\frac{\partial T}{\partial x}+v\frac{\partial T}{\partial y}\right)=\frac{\partial}{\partial y}\left(k\frac{\partial T}{\partial y}\right)+\mu\left(\frac{\partial u}{\partial y}\right)^2-\frac{\partial q_r}{\partial y} \tag{3}$$

$$u\frac{\partial C}{\partial x}+v\frac{\partial C}{\partial y}=D\frac{\partial^2 C}{\partial y^2} \tag{4}$$

with boundary conditions

$$u=u_w+L\frac{\partial u}{\partial y},\ v=-v_0,\ -k\frac{\partial T}{\partial y}=h_w(T_w-T),\ C=C_w \text{ for } y=0 \tag{5}$$

$$u\to u_\infty,\ T\to T_\infty,\ C\to C_\infty \text{ for } y\to\infty \tag{6}$$

where u and v are velocities in the direction of x and y-axis respectively, L represents slip length, thermal conductivity is k, fluid density is ρ, coefficient of viscosity is μ,specific heat a constant pressure is Cp, q_r is radiative heat flux, T is temperature, mass diffusivity is D and $h_w$is convective heat transfer and consideration the following dimensionless variables for the above equations (1)-(4) [19], where kinematic viscosity of an ambient fluid denoted by $\vartheta_\infty=\frac{\mu_\infty}{\rho}$. The geometrical interpretation are given as below in figure 1.

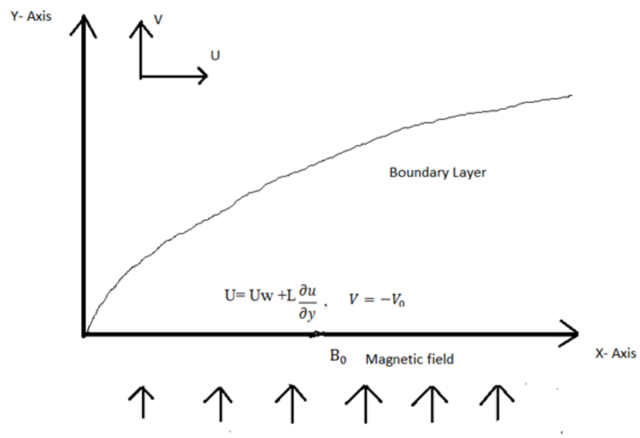

Fig. **1 Geometry of the considered Problem**

The mathematical analysis of the problem is simplify via by means of similarity transforms. Equations (1) - (4) alongcorresponding boundary conditions (5) - (6), are transformed by appropriate similarity transformations aregiven as follows:

$\eta = y\sqrt{\frac{U_\infty}{\vartheta_\infty x}}$,$\Psi$=$\sqrt{U_\infty \vartheta_\infty x}f(\eta)$, $\theta(\eta)$=$\frac{T-T_\infty}{T_w-T_\infty}$, $\phi(\eta)$=$\frac{C-C_\infty}{C_w-C_\infty}$

(7)

The equations of continuity hold good by using a stream function $\Psi(x,y)$ such that.

$u = \frac{\partial \Psi}{\partial y}, v = -\frac{\partial \Psi}{\partial x}$ and $u = U_\infty f'(\eta), v = \frac{1}{2}\sqrt{\frac{\vartheta_\infty U_\infty}{x}}(f - \eta f')$ (8)

Where q_r is the radiative heat flux in the x-direction is notmeasured in comparison to the y-direction. By,Rosseland approximation for radiation q_r is given as follows [19].

$q_r = -\frac{4\sigma^*}{3k^*}\frac{\partial T^4}{\partial y}$

(9)

WhereStefan-Botlzmann constant and mean absorption coefficient are defined as $\sigma^*$and k^*respectively.

Theflow temperature difference is adequately small in such a manner that the term T^4 is a linear function of temperature inside the flow. The Taylor series expansion about a free stream temperature T_∞ for $T^4$is given by [19].

$T^4 = T_\infty^4 + 4T_\infty^3(T - T_\infty) + 6T_\infty^2(T - T_\infty)^2 + \ldots\ldots$ (10)

Equation (10) can be re-write as follows, after neglecting higher-order terms beyond the first order in $(T - T_\infty)$,

$T^4 \approx 4T_\infty^3 T - 3T_\infty^4$ (11)

Here μ is fluid dynamic viscosity which is an inverse linear function of temperature and denoted as

$\frac{1}{\mu} = \frac{1}{\mu_\infty}[1 + \chi(T - T_\infty)]$ (12)

Wheredynamic viscosityat ambient temperature is given by $\mu_\infty$and χ as the thermal property of liquid. Equation (12) can be re-written as follows.

$\frac{1}{\mu} = a(T - T_r)$ (13)

Where $a = \frac{c}{\mu_\infty}$and $T_r = T_\infty - \frac{1}{\chi}$are constants and define the dimensionless values are a function of reference state and thermal property of liquid. A definite model of variable thermal conductivity obtained as.

$k = k_\infty(1+\varepsilon\frac{T-T_\infty}{\Delta T})$ (14)

Where thermal conductivity at ambient temperature is denoted by k_∞,$\Delta T = T_w - T_\infty$and ε is thermo-physical constant depend on liquid ε< 0 for lubrication and hydromagnetic working liquidsε> 0 for water and equation (14) can be obtained as follows,

$k = k_\infty(1+\varepsilon\theta)$ (15)

The dimensionless form of temperature θ is

$$\theta = \frac{T - T_\infty}{T_\infty - T_w} + \theta_r$$
(16)

where $\theta_r = \frac{T_r - T_\infty}{T_w - T_\infty} = -\frac{1}{\delta(T_w - T_\infty)}$ and the value is obtained by the viscosity characteristics of the liquid in consideration and the difference in operating temperatures. The value of θ_r is large, with $T_w - T_\infty$ is small. Flow is free from variable viscosity effect. On the other hand, for small θ_r either, the viscosity of the liquid changes with temperature, or the operating temperature difference is significant. Notice that the value of θ_r is negative for liquids [20].

By using the equations (14) and (16), the following equation

$$\mu = \mu_\infty \left(\frac{\theta_r}{\theta_r - \theta}\right)$$
(17)

By using transformation equation (7) the converted coupled nonlinear ordinary differential equation is given as follows:

$$\left(\frac{\theta_r}{\theta_r - \theta}\right) f''' + \frac{f f''}{2} + \frac{\theta_r}{(\theta_r - \theta)^2} f'' \theta' - M^2 (f' - 1) = 0 \qquad (18)$$

$$(1 + \varepsilon\theta + Nr)\theta'' + \varepsilon\theta'^2 + \square\square\square\square \left(1 - \frac{\theta}{\square_\square}\right)(1 + \square\square)\square''^2 + \left(1 - \frac{\theta}{\square_\square}\right)(1 + \square\square)\frac{\square\square\square\square'}{2} = 0 \qquad (19)$$

$$\square'' + \frac{\square\square\square\square'}{2} = 0 \qquad (20)$$

with the corresponding boundary conditions

$$\square = \square_\square,\ \square' = \square + \square\square'',\ \square' = -\square\left(\frac{1 - \square(0)}{1 + \square\square(0)}\right), \square(0) = 1 \text{ for } \eta \to 0.$$

$$f'(\eta) \to 1, \theta(\eta) \to 0, \phi(\eta) \to 0 \text{ as } \eta \to \infty.$$

Where prime denotes the derivative of variable with respect to η.Where η is the function of two variables x, y. The governing parameters are presented as follows:

$M = B_0\sqrt{\frac{\sigma x}{\rho U_\infty}}$(Magnetic Parameter), $Pr = \frac{\vartheta}{\alpha}$(Prandtl Number), $Nr = \frac{16 T_\infty^3 \sigma^*}{3k^* k_\infty}$(Radiation Parameter), $\delta = L\sqrt{\frac{U}{\vartheta x}}$ (Slip parameter), $\lambda = \frac{U_w}{U}$ (Velocity ratio Parameter), $Ec = \frac{u^2}{C_p \Delta T}$(Eckert Number), $Sc = \frac{\vartheta}{D}$(Schmidt Number), $a = \frac{h_w}{k_\infty\sqrt{\frac{\vartheta x}{U}}}$ (Surface convection Parameter)

Here$B(x)$represents applied magnetic field andconvective heat transfer denoted h_w and both are function of $x^{\frac{-1}{2}}$. It is assumed that $B(x) = B_0 x^{\frac{-1}{2}}$, $h_w = cx^{\frac{-1}{2}}$, where B_0 and c are constants. In the case of the flow of liquids, slip parameter δ can be defined as follows.

$$\delta = Kn_{x,L}\sqrt{Re_x} \qquad (21)$$

where the Kundsen number $Kn_{x,L}$ is depends on$L$which represents the slip length and Re_x indicateslocal Reynolds number follows:

$$Kn_{x,L} = \frac{L}{x},\ Re_x = \frac{Ux}{\vartheta}$$

It's worth noting that because of the parameter $\delta(x)$, the liquid doesn't develop self-similar solutions. Also, the across the boundary layer viscosity and thermal conductivity also change. Pr also varies, and the relation between Prandtl number and ambient Prandtl number is as follows.

$$\Pr = \frac{\mu C_p}{k} = \frac{\left(\frac{\theta_r}{\theta_r - \theta}\right)\mu_\infty Cp}{k_\infty(1 + \varepsilon\theta)} = \frac{1}{\left(1 - \frac{\theta}{\theta_r}\right)(1 + \varepsilon\theta)} Pr_\infty$$

Where Pr_∞ is ambient Prandtl number. The values of engineering interest that are denoted in this way are the skin friction coefficient (rate of shear stress), nusselt number (rate of heat transfer), and sherwood number (rate of mass transfer).

$C_f = \frac{2\tau}{\rho u^2}$ where $\tau = \mu \left(\frac{\partial u}{\partial y}\right)_{y=0}$ Hence $C_f = 2Re_x^{\frac{-1}{2}} \left(\frac{\theta_r}{\theta_r - \theta}\right) f''(0)$

The local Nusselt number is denoted as

$Nu_x = \frac{xq_w}{(T - T_\infty)}$ the heat flux is given by $q_w = -k \left(\frac{\partial T}{\partial y}\right)_{y=0}$, $Nu_x = \frac{1}{2}\sqrt{Re_x}\frac{1}{\theta(0)}$ or

$Nu_x^* = \theta(0)$ where $Nu_x^* = \frac{1}{2}\sqrt{Re_x} Nu_x^{-1}$, Also local Sherwood number is followed by $Sh^* = -\phi'(0)$. Physical parameters numerically obtained as C_f^*, Nu_x and Sh^* respectively.

NUMERICAL APPROACH

The effects of thermophysical properties on convective heat transfer on mhd slip flow with non-linear coupled ordinary differential equations were investigated in this study using a proficient 4thRunge-Kutta method and shooting method ODE45 solver for equations (18)-(20) with various parameters Pr, Ec, M, Nr, Sc, θ_r, ε.The system of first-order seven differential equations is used to transform the non-linear governing ordinary differential equations. Momentum, energy, and concentration equations in f are third-order, θ and ϕ second-order respectively. To solve the system of equations, this technique required seven boundary conditions, but only four are available in this case: two initial conditions for f and a single condition for both θ and ϕ, respectively. The values at ambient conditions have already been provided, i.e. $\eta \to \infty$,When adopting the shooting method, the ambient position plays a critical role in generating the unknown initial $\eta = 0$.The boundary value problem is solved by using equations (18)-(20) to obtain $f''(0), \theta'(0)$, $\phi'(0)$.Solution technique is repetitive with a larger value of until just the requisite significant digit differences between two successive values of $f''(0), \theta'(0)$, $\phi'(0)$.Inside the boundary layer, the last value is regarded a finite number for the various physical parameters for f', θ and ϕ. Then a system of seven simultaneous first-order differential equations with seven unknowns was used to condense a coupled third-order boundary layer value issue in f, θ and ϕ second order.

The equations (18)-(20) can be expressed as follows.

$$f''' = \left(\frac{\theta_r - \theta}{\theta_r}\right)\left(-\frac{ff''}{2} - \frac{\theta_r}{(\theta_r - \theta)^2} f''\theta' + M^2(f' - 1)\right) \tag{22}$$

$$\theta'' = -\frac{1}{(1 + \varepsilon\theta + Nr)}\left(\varepsilon\theta'^2 + Ec\,Pr\left(1 - \frac{\theta}{\theta_r}\right)(1 + \varepsilon\theta)f''^2 + \left(1 - \frac{\theta}{\theta_r}\right)(1 + \varepsilon\theta)\frac{Prf\theta'}{2}\right) \tag{23}$$

$$\phi'' = -\frac{Scf\phi'}{2} \tag{24}$$

Defined new variables as follows:

$$y_1 = f,\ y_2 = f',\quad y_3 = f'',\quad y_4 = \theta,\ y_5 = \theta',\quad y_6 = \phi,\ y_7 = \phi'. \tag{25}$$

The following equations can be used to convert inhighly non-linear coupleddifferential equations along with the corresponding boundary conditions into seven equivalent first order differential equations.

$$y_1' = y_2$$

$$y_2' = y_3$$

$$y_3' = \left(1 - \frac{y_4}{\theta_r}\right)\left(-\frac{y_1 y_3}{2} - \frac{\theta_r\, y_3\, y_5}{(\theta_r - y_4)^2} + M^2(y_2 - 1)\right)$$

$y_4{}' = y_5$

$y_5{}' = -\frac{1}{(1+\varepsilon\, y_4+Nr\,)}\left(\varepsilon\, y_5{}^2 + EcPr\left(1-\frac{y_4}{\theta_r}\right)(1+\varepsilon\, y_4)y_3^2 + \left(1-\frac{y_4}{\theta_r}\right)(1+\varepsilon\, y_4)\frac{Pry_1\, y_5}{2}\right)$

$y_6{}' = y_7$

$y_7{}' = -\frac{Scy_1\, y_7}{2}$

Prime sign indicates differentiation with respect to η, and appropriate boundary conditions written in that manner.

$y_1(0) = f_w$, $y_2(0)=\lambda + \delta y_3(0)$, $y_3(0) = A$, $y_4(0) = B$, $y_5(0) = -a\left(\frac{1-y_4(0)}{1+\varepsilon y_4(0)}\right)$, $y_6(0) = 1$, $y_7(0) = C$.

Where are A, B,C assumed valued to get the solution.This approach converts a boundary value problem into an initial value problem (IVP). Then IVP is solved by assuming the omitted beginning value for parameters via an efficient shooting technique.The results are obtained represented by tables and graphically. Also, main features are analyzed and discussed.

RESULT AND DISCUSSION

The obtained numerical and graphical results are discussed in this section as follows.

The comparison between [9], [14] and [23] for the values of $-\theta'(0)$ calculated for various values of Pr and a when M=0, Nr =0, Sc =0, Ec =0, λ =0, ε =1,θ_r →∞ with $f_w = 1$ shows in Table 1.By table, it can be pragmatic that the represented solution is better than the existing literature results.

Table 1. $-\theta'(0)$ for various values of a and Pr when M=0, Nr=0, Sc=0, Ec=0, λ=0, ε =1,θ_r →∞ with $f_w = 1$.

a	Existed literature results						Present results	
	Pr=0.1 [9]	Pr=0.72 [9]	Pr =0.1 [14]	Pr =0.72 [14]	Pr =0.1 [23]	Pr =0.72 [23]	Pr =0.1	Pr=0.72
0.05	0.0373	0.0428	0.036900	0.042781	0.036844	0.042767	0.0297	0.0373
0.10	0.0594	0.0747	0.058423	0.074757	0.058339	0.074724	0.0423	0.0596
0.20	0.0848	0.1193	0.082477	0.119358	0.082365	0.119295	0.0537	0.0850
0.40	0.1076	0.1700	0.103865	0.170089	0.103722	0.169994	0.0621	0.1079
0.60	0.1182	0.1981	0.113688	0.198155	0.113536	0.198051	0.0655	0.1186
0.80	0.1243	0.2159	0.119329	0.215976	0.119174	0.215864	0.0673	0.1247
1	0.1283	0.2282	0.122999	0.228303	0.122833	0.228178	0.0685	0.1287
5	0.1430	0.2791	0.136400	0.279283	0.136219	0.279131	0.0725	0.1437
10	0.1450	0.2871	0.138279	0.287291	0.138100	0.287146	0.0730	0.1455
20	0.1461	0.2913	0.139242	0.291478	0.13906	0.291329	0.0732	0.1470

Table 2. Values of $f''(0)$, $\theta(0)$,$-\theta'(0)$ and $-\phi'(0)$ for various values of θ_r,ε and a for Pr=1, M=1, Nr=1, Sc =2, Ec=1 and λ=-0.2.

Parameter			δ=0				δ=0.5			
θ_r	ε	a	$f''(0)$	$\theta(0)$	$-\theta'(0)$	$-\phi'(0)$	$f''(0)$	$\theta(0)$	$-\theta'(0)$	$-\phi'(0)$
3	0	0.01	2.7047	0.963261	0.9976	1.2263	2.1271	0.464605	0.0146	1.5884
		0.5	2.6874	0.984768	0.0207	1.2239	2.0116	0.782591	0.2955	1.5531
		1	2.6828	0.990466	0.0259	1.2233	1.9790	0.865060	0.3668	1.5430

		1.5	2.6807	0.993062	0.0283	1.2230	1.9640	0.902217	0.3987	1.5382
	1	0.01	2.7047	0.963261	0.5083	1.2263	2.1271	0.464605	0.0099	1.5884
		0.5	2.6874	0.984768	0.0104	1.2239	2.0116	0.782591	0.1658	1.5531
		1	2.6828	0.990466	0.0130	1.2233	1.9790	0.865060	0.1967	1.5430
		1.5	2.6807	0.993062	2.0458	1.2230	1.9640	0.902217	0.2096	1.5382
5	0.2	0.01	2.9657	1.002231	0.5051	1.2642	2.1857	0.460787	0.0134	1.6066
		0.5	2.9662	1.000975	0.0011	1.2643	2.1257	0.765588	0.2763	1.5889
		1	2.9664	1.000620	0.0014	1.2643	2.1083	0.850559	0.3472	1.5836
		1.5	2.9965	1.000454	0.7394	1.2643	2.1083	0.890238	0.3799	1.5836
∞	0.2	0.01	3.3505	1.104846	0.0137	1.3147	2.2648	0.465134	0.0133	1.6307
		0.5	3.3505	1.044130	0.0594	1.3147	2.2648	0.765983	0.2758	1.6307
		1	3.3505	1.027703	0.0622	1.3147	2.2648	0.850324	0.3477	1.6307
		1.5	3.3505	1.020184	0.0820	1.3147	2.2648	0.889870	0.3812	1.6307
∞	0	0.01	3.3505	1.145620	0.0039	1.1924	2.2648	0.472466	0.0143	1.6307
		0.5	3.3505	1.055680	0.0757	1.1924	2.2648	0.783083	0.2948	1.6307
		1	3.3505	1.034154	0.0928	1.1924	2.2648	0.864497	0.3683	1.6307
		1.5	3.3505	1.024632	0.1004	1.1924	2.2648	0.901475	0.4017	1.6307

It can be observed that from Table 2 When the surface convection parameter (a) is increased, skin friction coefficient $(f''(0))$ and rate of heat transfer $(-\theta'(0))$ decline whereas rate of mass transfer number $(-\phi'(0))$ increases. When thermal conductivity parameter (ε) is increased, the $(f''(0))$ increases, while $(-\theta'(0))$ and $(-\phi'(0))$ decrease. Furthermore, variable viscosity parameter $((\theta_r)$ has the effect of decreasing $(f''(0))$ and $(-\phi'(0))$ while increasing $(-\theta'(0))$.Finally, the $(f''(0))$, $(-\theta'(0))$ and $(-\phi'(0))$ drop as slip parameter (δ) enhanced.The impact of surface convection parameter (a)on velocity profile presented in fig. 2. Velocity profile increases when a increases.

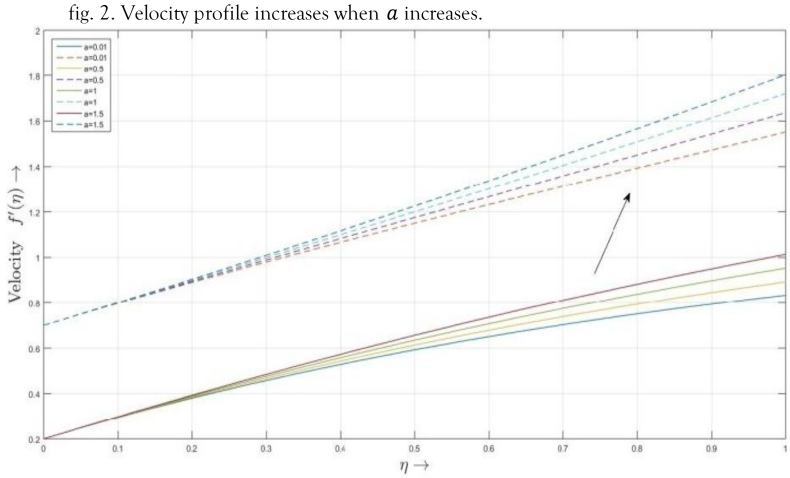

Fig. **2** $f'(\eta) Vs\, \eta$**for different** a

The role of Eckert number Ec on velocity is shown in fig. 3. From this figure, it is analyzed that velocity increases while Ec increases.

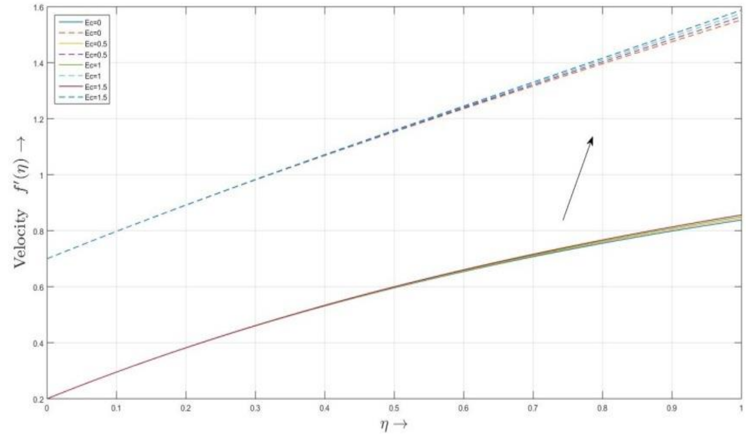

Fig. **3** $\boldsymbol{f'(\eta) Vs\,\eta}$ **for different** $\boldsymbol{Ec}$

fig. 4 and fig.5 indicate the effect of velocity ratio parameter λ for λ >0 and λ<0 on velocity profile, respectively. It is analyzing that with the increase in λ (positive and negative) the velocity enhanced.

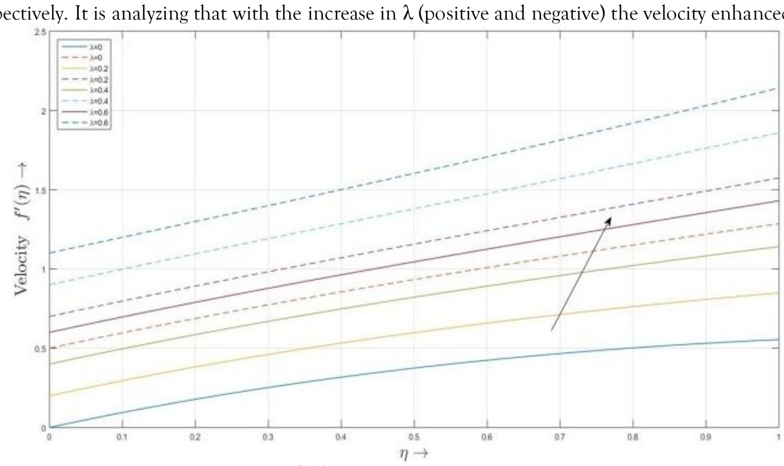

Fig. **4** $\boldsymbol{f'(\eta) Vs\,\eta}$ **for different** $\boldsymbol{\lambda}$ **(Positive)**

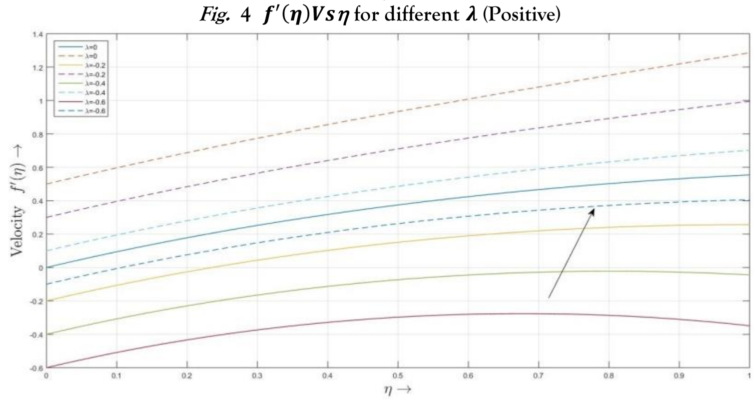

Fig. **5** $\boldsymbol{f'(\eta)\ Vs\,\eta}$ **for different** $\boldsymbol{\lambda}$ **(Neagative)**

Fig. 6 and 7 represents the role of variable viscosity parameter θ_r on velocity and temperature distributions. It can be seen in these graphs that when the θ_r grows, the velocity and temperature profile drops and increases respectively.

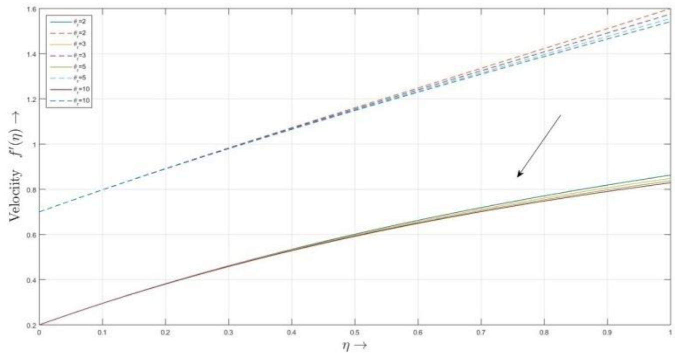

Fig. **6** $\boldsymbol{f'(\eta)}$ $\boldsymbol{Vs\,\eta}$ **for different** $\boldsymbol{\theta_r}$ **(Positive)**

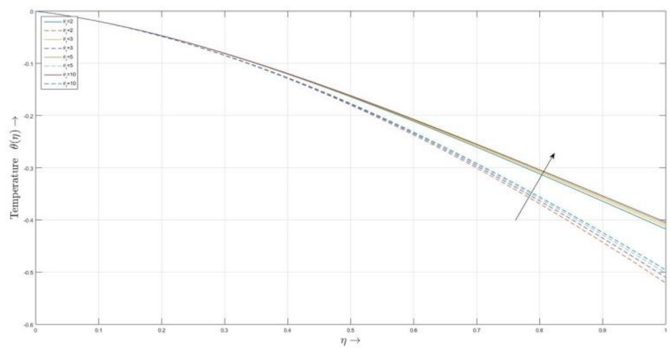

Fig. **7** $\boldsymbol{\theta(\eta) Vs\,\eta}$**for different**$\boldsymbol{\theta_r}$ **(Positive)**

fig. 8 and fig. 9 indicate the velocity and temperature profile for variable viscosity parameter $-\theta_r$, respectively. As the value of $-\theta_r$ enlarges then velocity and temperature reduces.

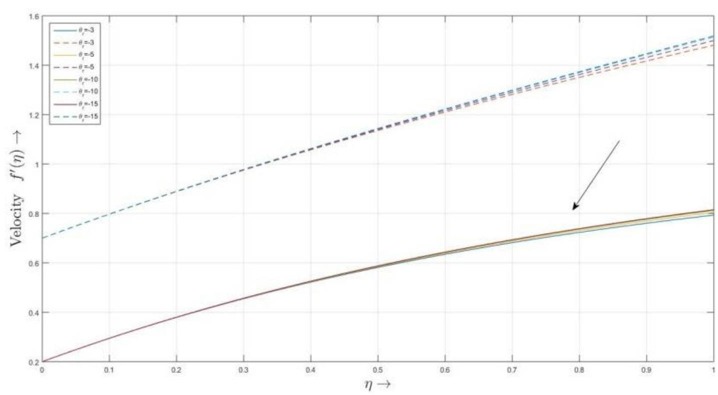

Fig. **8** $\boldsymbol{f'(\eta) Vs\,\eta}$ **for different**$\boldsymbol{\theta_r}$ **(Negative)**

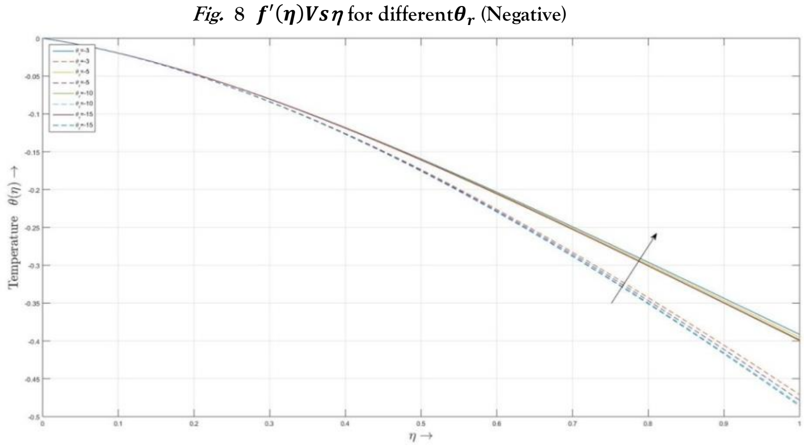

Fig. **9** $\boldsymbol{\theta(\eta)}$ $\boldsymbol{Vs\ \eta}$ **for different** $\boldsymbol{\theta_r}$ **(Negative)**

fig. 10 indicates the role of variable thermal conductivity ε on velocity profile. As the ε rises, so does the velocity profile. Because ε rises, momentum boundary layer thickness rises as well, hence the velocity distribution improved.

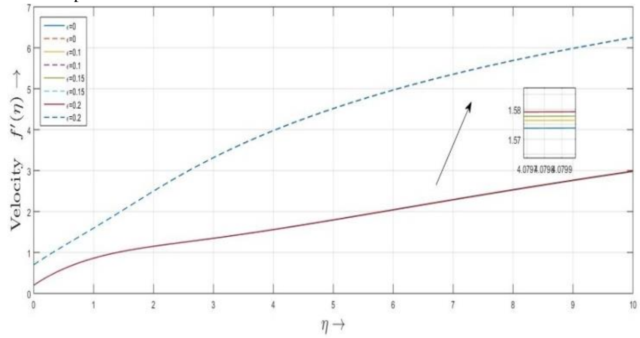

Fig. 10 $\boldsymbol{f'(\eta)}$ $\boldsymbol{Vs\,\eta}$ **for different** $\boldsymbol{\varepsilon}$

The analysis of Hartmann number Mon velocity and temperature distributionillustrated in fig. 11 and 12. It is analyze that increasing, M causes the velocity reduces while temperature profile increases respectively. It demonstrates that momentum is ebbing due to Lorentz forces that can act against the flow. and as M increases the thickness of corresponding thermal layer increases.Because applied magnetic field transfer heat to the fluid, heat transfer from the plate is reduced. Which results to increase in temperature.

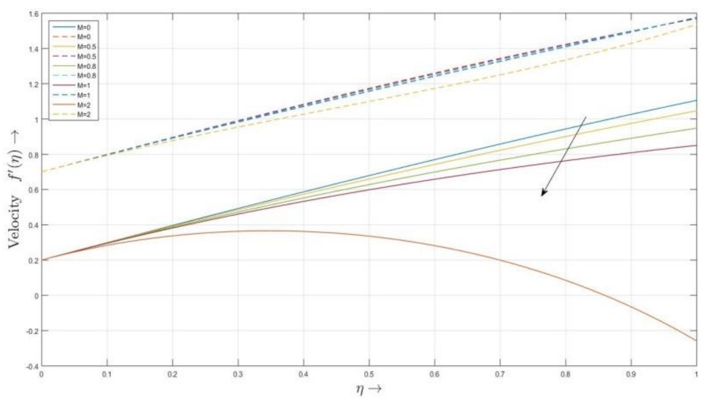

Fig. 11 $\boldsymbol{f'(\eta)}$ $\boldsymbol{Vs\ \eta}$**for different** $\boldsymbol{M}$

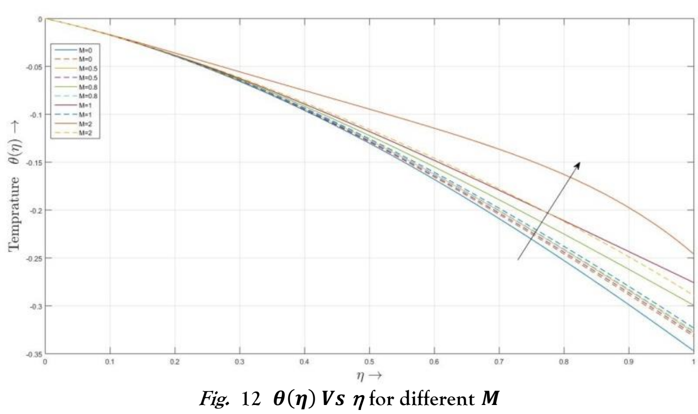

Fig. 12 $\boldsymbol{\theta(\eta)}$ $\boldsymbol{Vs\ \eta}$ **for different** $\boldsymbol{M}$

Impactof radiation parameter Nr on velocity and temperature profile illustrated in fig. 13 and14. From the graphs show that as the Nr is increased, the velocity profile reduces but the temperature distribution grows. Furthermore, the temperature profile reveals that as the Nr is increased,As the rate of heat transfer to the fluid increases, the temperature of the fluid rises.

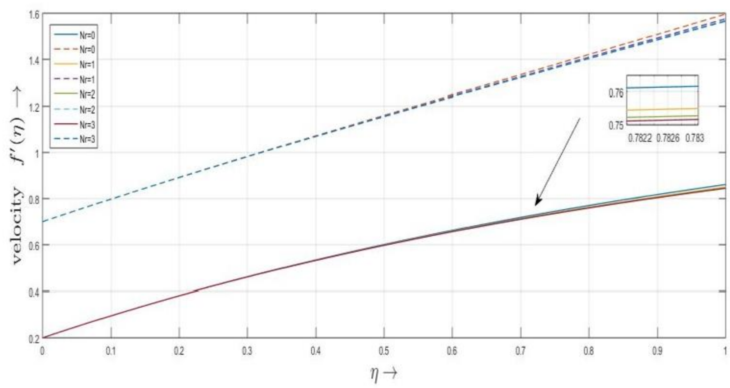

Fig. 13 $\boldsymbol{f'(\eta)}$ $\boldsymbol{Vs}$ $\boldsymbol{\eta}$ **for different** $\boldsymbol{Nr}$

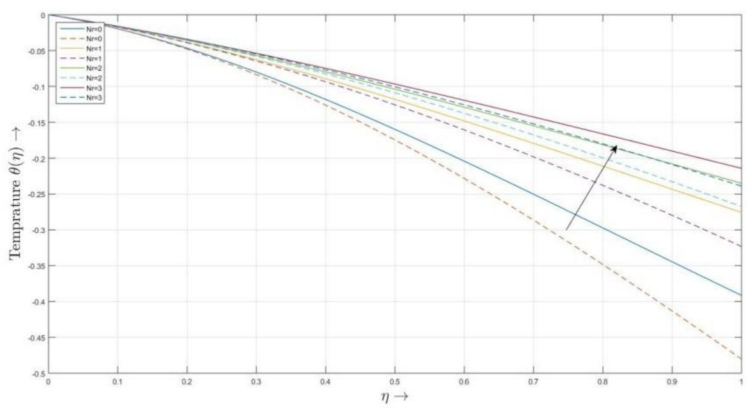

Fig. 14 $\boldsymbol{\theta(\eta)}$ $\boldsymbol{Vs}$ $\boldsymbol{\eta}$ **for different** $\boldsymbol{Nr}$

The impact of prandtl number Pr on velocity and temperature profile indicated in fig. 15 and16. These figures show that increasing Pr increases velocity profile while decreasing temperature distribution. An increase in the Pr by definition, indicates a slow rate of thermal diffusion and temperature profile drops.

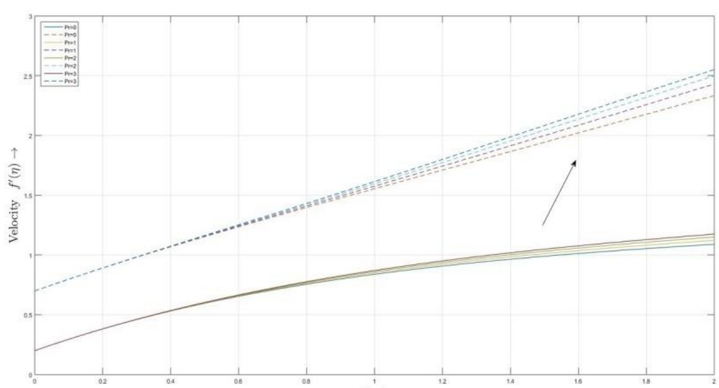

Fig. 15 $\boldsymbol{f'(\eta)}$ $\boldsymbol{Vs}$ $\boldsymbol{\eta}$ **for different** $\boldsymbol{Pr}$

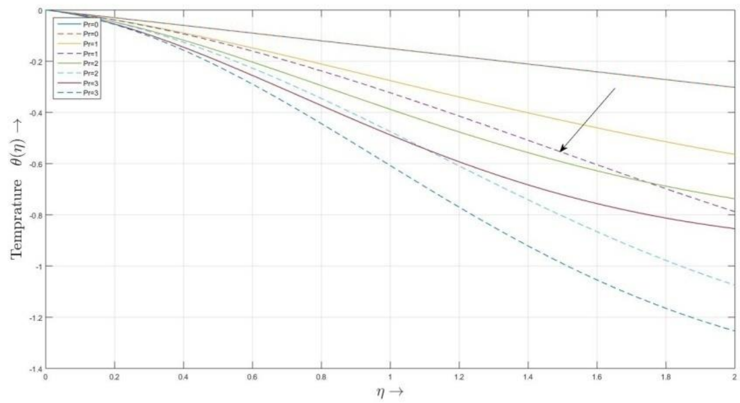

Fig. 16 $\boldsymbol{\theta(\eta)}$ $\boldsymbol{Vs}$ $\boldsymbol{\eta}$**for different** $\boldsymbol{Pr}$

The behavior of surface convection parameter a on temperature distribution is represented in fig. 17. It is analyzed that the increase in a which results to decline in temperature profile.

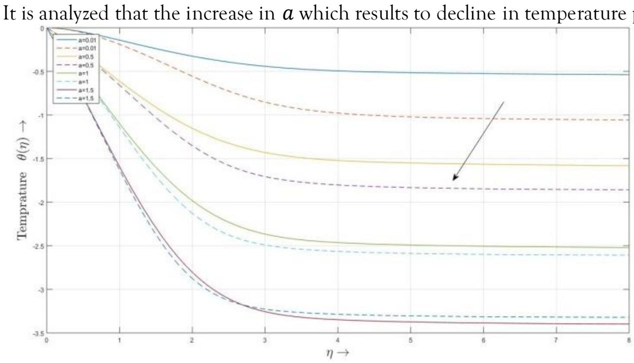

Fig. 17 $\boldsymbol{\theta(\eta)}$ $\boldsymbol{Vs}$ $\boldsymbol{\eta}$ **for different** $\boldsymbol{a}$

The impact of Eckert numberEc on temperature distributionillustrated in fig. 18. As the increase inEc causes, the temperature profile decreases.

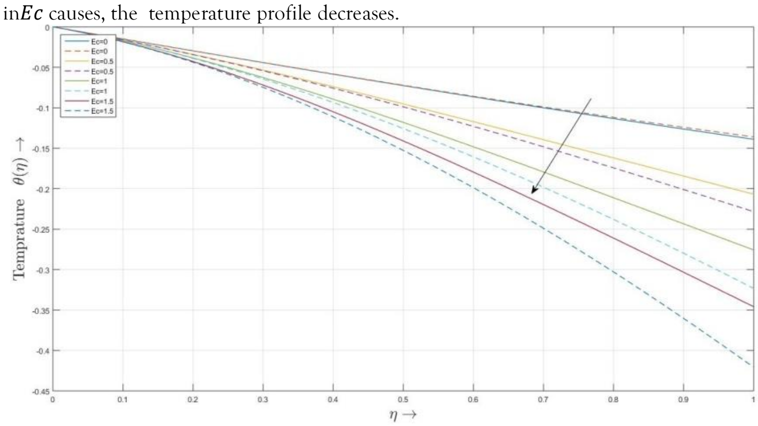

Fig. 18 $\boldsymbol{\theta(\eta)}$ $\boldsymbol{Vs}$ $\boldsymbol{\eta}$**for different** $\boldsymbol{Ec}$

The impact on temperature profile with variable thermal conductivity $\varepsilon$is depicted in fig. 19. Temperature profile decline as ε rises.As thermal boundary layer thicknessreduced with the enhancement in ε.Therefore, the temperature profile drops.

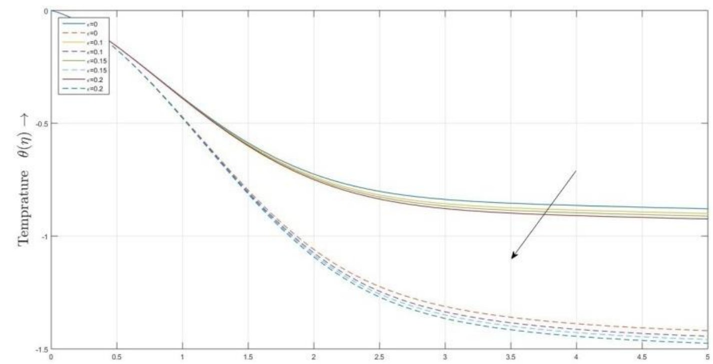

Fig. 19 $\boldsymbol{\theta(\eta)}$ $\boldsymbol{Vs}$ $\boldsymbol{\eta}$**for different** $\boldsymbol{\varepsilon}$

fig. 20 and fig. 21 indicate the impactof velocity ratio parameter λ for λ> 0 and λ< 0 cases on temperature profile, respectively. Here the effect of λ greatly affects the temperature. The temperature profile elevates as λ> 0 increases. Whereas the temperature profile decline as λ< 0 increases.

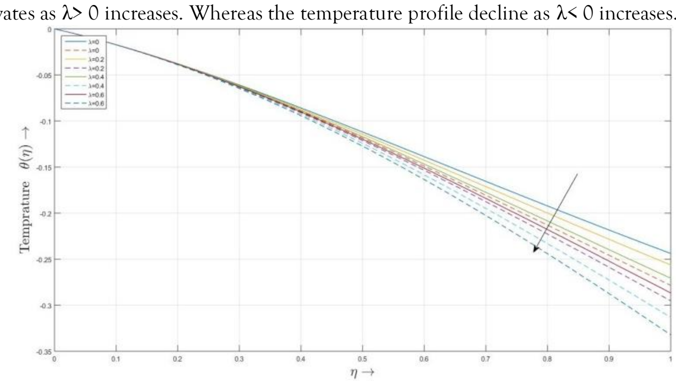

Fig. 20 $\boldsymbol{\theta(\eta)}$ $\boldsymbol{Vs}$ $\boldsymbol{\eta}$**for different** $\boldsymbol{\lambda}$ **(Positive)**

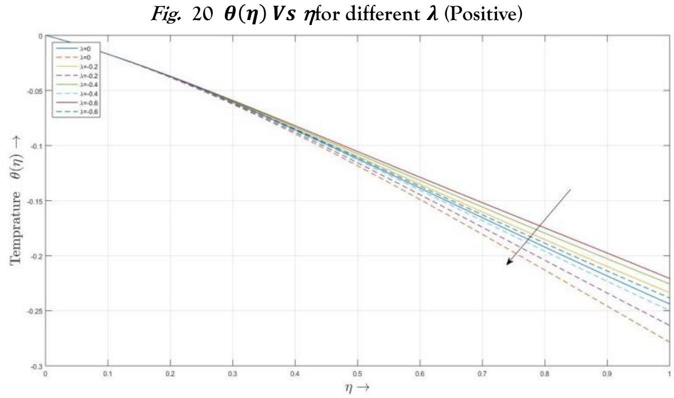

Fig. 21 $\boldsymbol{\theta(\eta)}$ $\boldsymbol{Vs}$ $\boldsymbol{\eta}$**for different** $\boldsymbol{\lambda}$ **(Negative)**

The role of radiation parameter Nron concentration profile illustrated in fig. 22. It analyze that with the increasing in Nr causes the concentration profile increases.

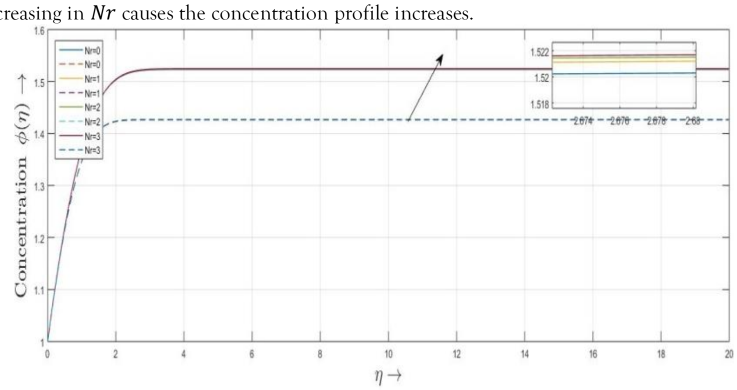

Fig. 22 $\boldsymbol{\phi(\eta) Vs \eta}$**for different** $\boldsymbol{Nr}$

The effect of Eckert number Econ concentration is illustrated in fig. 23. The results indicates that the increase in Ec gives to an increase in solute concentration. Therefore, the concentration profile was reduced. The impact of Ec on concentration is non-similar in comparison to temperature profile.

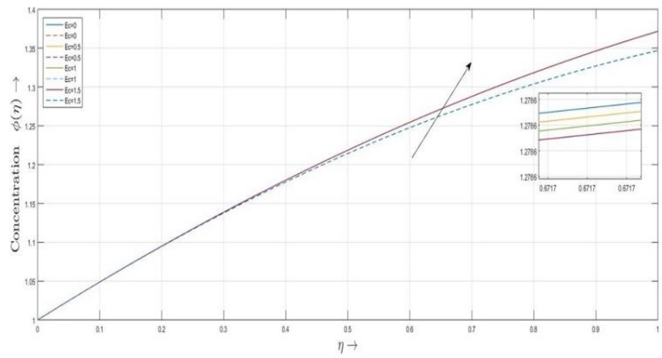

Fig. **23** $\boldsymbol{\phi(\eta)}$ $\boldsymbol{Vs}$ $\boldsymbol{\eta}$**for different** $\boldsymbol{Ec}$

fig. 24 indicates the role of variable thermal conductivity ε on concentration profile. Impact of ε on concentration distribution is reversed, whereas ε= 0 implies constant thermal conductivity.

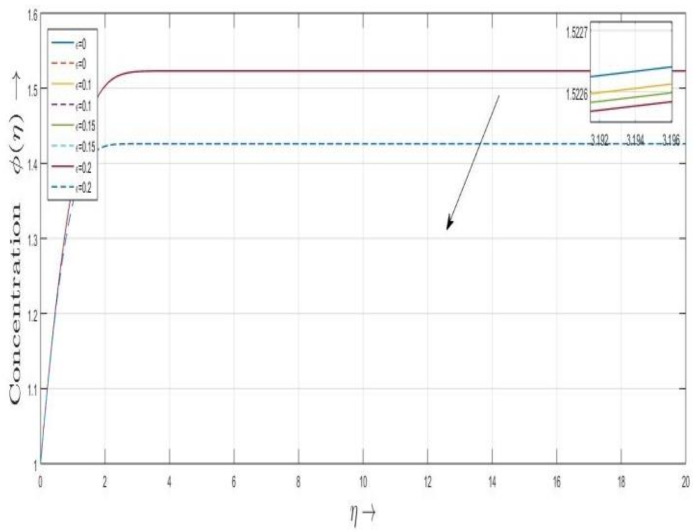

Fig. **24** $\boldsymbol{\phi(\eta)}$ $\boldsymbol{Vs}$ $\boldsymbol{\eta}$**for different** $\boldsymbol{\varepsilon}$

fig. 25 and 26 show the results for the velocity ratio parameter λ on concentration. It is indicated from these figures that with the increase in λ for λ> 0 and λ< 0 decrease in concentration profile.

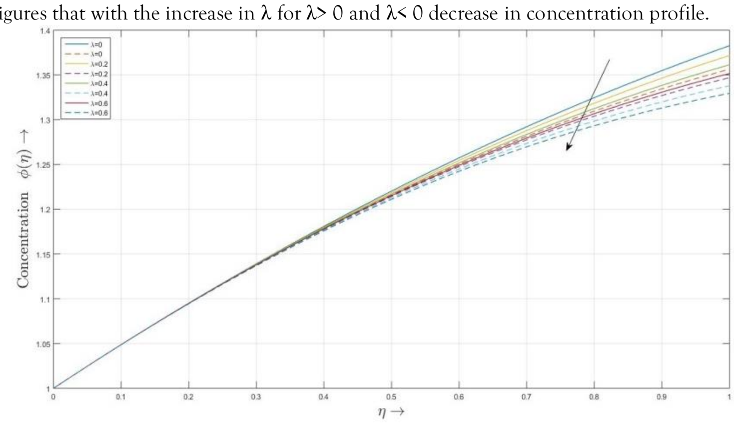

Fig. **25** $\boldsymbol{\phi(\eta)}$ $\boldsymbol{Vs}$ $\boldsymbol{\eta}$**for different** $\boldsymbol{\lambda}$ **(Positive)**

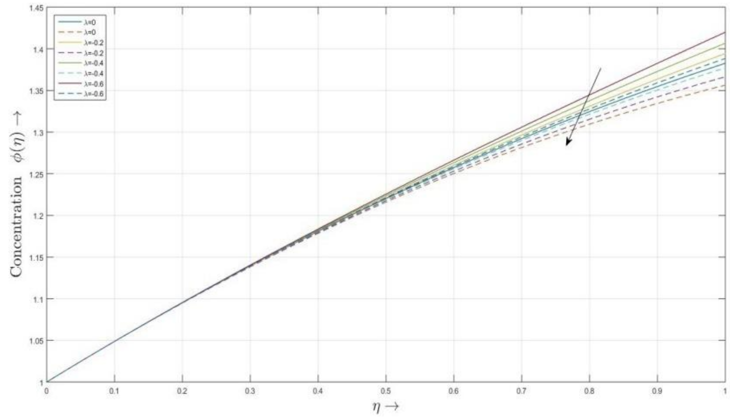

Fig. **26 $\boldsymbol{\phi(\eta)}$ $\boldsymbol{Vs}$ $\boldsymbol{\eta}$for different $\boldsymbol{\lambda}$(Negative)**

fig. 27 indicates the role of magnetic parameter M on concentration profile.Thesolute concentration rises forhigher values of M. Therefore concentration profile increases.

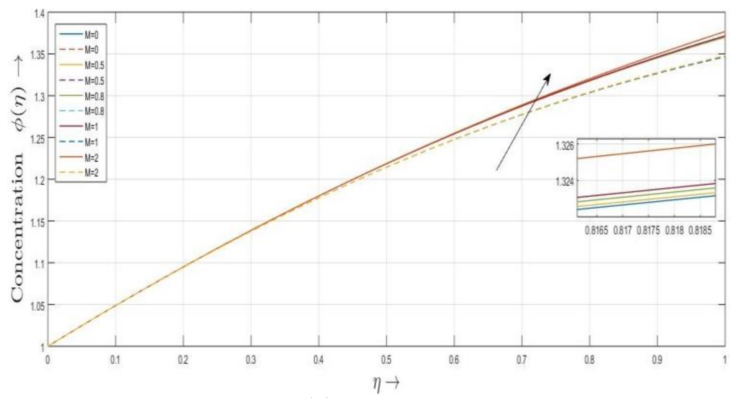

Fig. **27 $\boldsymbol{\phi(\eta)}$ $\boldsymbol{Vs}$ $\boldsymbol{\eta}$for different $\boldsymbol{M}$**

The behavior of Schmidt number Sc on concentration distribution discussed in fig. 28. As the Schmidt number Sc enlarges, the solutaldistribution reduces. With the increase in Sc, by definition, indicates a slow rate of mass diffusion. As a result, the concentration profile is reduced.

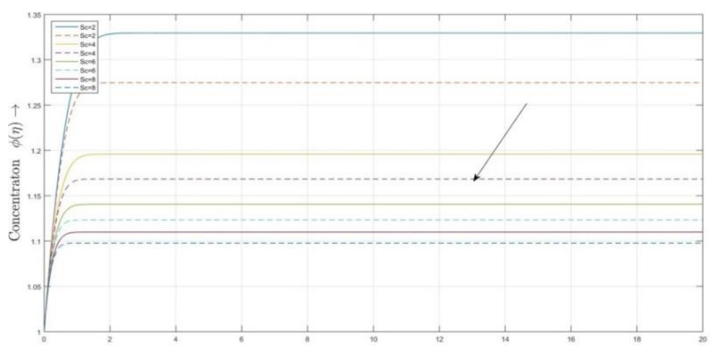

Fig. **28 $\boldsymbol{\phi(\eta)}$ $\boldsymbol{Vs}$ $\boldsymbol{\eta}$for different $\boldsymbol{Sc}$**

fig. 29 depict the impact of Prandtl number Pr on concentration profile. It is analyzed that with the rise in Pr brings a decrease to the concentration profile.

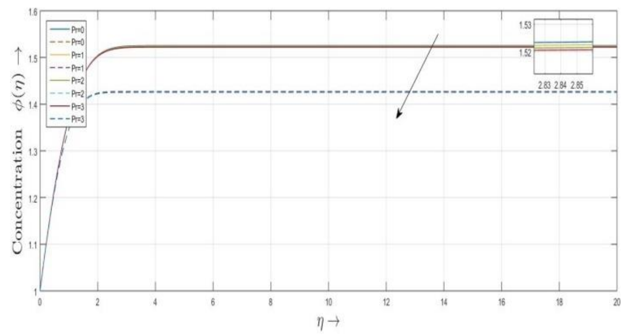

***Fig.* 29 $\boldsymbol{\phi(\eta)}$ $\boldsymbol{Vs}$ $\boldsymbol{\eta}$ for different $\boldsymbol{Pr}$**

fig. 30 shows the role of surface convection parameter (a) on concentration distribution. It is revealing that as increase in a reduces the concentration distribution.

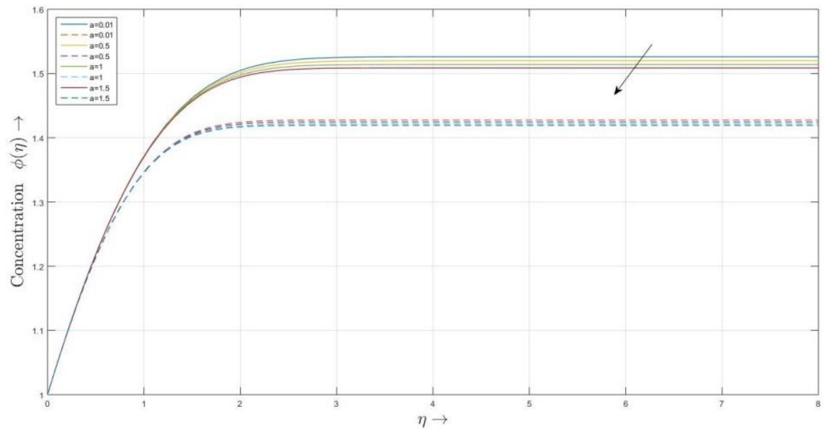

***Fig.* 30 $\boldsymbol{\phi(\eta)}$ $\boldsymbol{Vs}$ $\boldsymbol{\eta}$for different $\boldsymbol{a}$**

fig. 31 and fig. 32 indicate the influence of variable viscosityθ_r on concentration profile. Here influence of θ_r greatly affects the concentration. It is observed that an increasing in θ_r for θ_r> 0 and θ_r< 0 increases concentration profile.

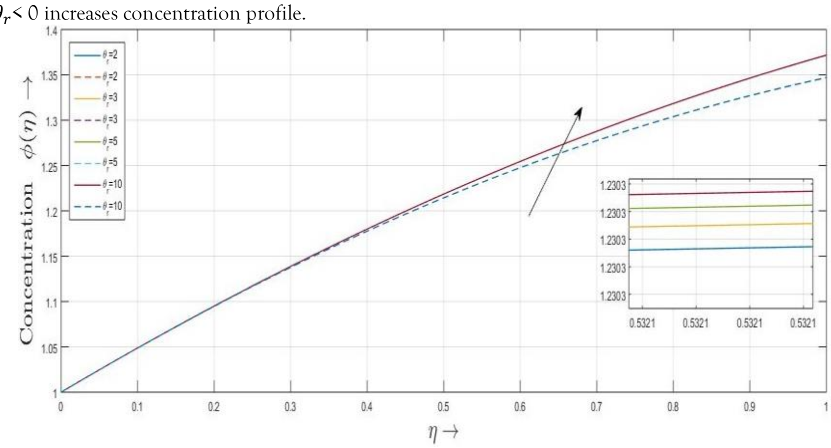

***Fig.* 31 $\boldsymbol{\phi(\eta)}$ $\boldsymbol{Vs}$ $\boldsymbol{\eta}$for different $\boldsymbol{\theta_r}$(Positive)**

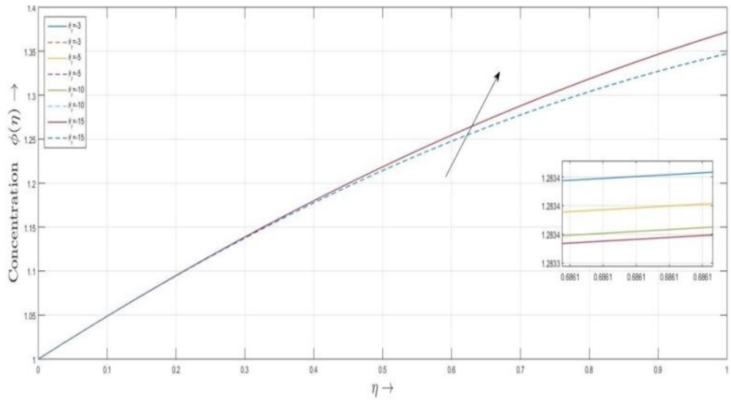

***Fig.* 32 $\boldsymbol{\phi(\eta)\ Vs\ \ \eta}$ for different $\boldsymbol{\theta_r}$(Negative)**

CONCLUSION

In order to analyze steady 2-D boundary layer MHD fluid flow over a permeable moving plate alongthermo-physical properties. The similarity transformations were used to derive the dimensionless boundary value problem. The governing equations of fluid flow governed by various prominent parameters like slip parameter (δ), radiation (Nr), Hartmann number (M), Schmidt number (Sc), Prandtl number (Pr), variable thermal conductivity (ε), variable viscosity (θ_r).Numerical solution is given by RungeKutta 4th order shooting technique with the help of the ODE45 solver. The key outcomes are listed below.

i. The velocity profile is decreased on increasing magnetic field M. Whereas velocity distribution decreases on the enhancement of variable viscosity parameter θ_r, for both positive and negative value of θ_r.
ii. The influence of variable thermal conductivity ε on velocity is that as ε increase, the velocity is also enhanced.
iii. The reverse trend is followed by temperature profile with surface convection parameter (a) i.e., as surface convection rises , the temperature profile becomes diminishes, but temperature profile increases in increment of value of θ_r. Whereas temperature profile becomes reduced as the thermal conductivity parameter ε is increased.
iv. The reverse trend is followed by ε i.e. as ε increases concentration profile is reduced. But for positive $\theta_r$concentration profile increased with increase in θ_r. And for - $\theta_r$the concentration profile is also increased.
v. As Schmidt number (Sc) decreases the concentration distribution.

The provided research work contributes new dimensions to the engineering field in determining the flow characteristic of hydrocarbon in oil and gas reservoirs, soil mechanics, groundwater in aquifers, chemical engineering (filtration). In these applications, the present solution provided help for solving permeable condition with variable fluid properties.The current simulations have been proven to be extremely useful in the investigation of engineered magnetic materials manufacturing. Despite the fact that the in the current study restricted on steadystate is only, but unstable state can be considered for future work.

References

[1]. H. I. Anderson, K.H. Bech, B.S. Dandapat, Magnetohydrodynamic flow of power-law fluid over a stretching sheet,International Journal of Non-linear Mechanics, 27(6) (1992) 929-936.
[2]. Yu. Shiping, T. A. Ameel, Slip-flow heat transfers in rectangular microchannels, International Journal of Heat and Mass Transfer, 44(2) (2001) 4225-4234.
[3]. A. J. Chamkha, Unsteady MHD convective heat and mass transfer past a semi-infinite vertical permeable moving plate with heat absorption, International journal of engineering science, 42(2) (2004) 217-230.
[4]. M. J. Martin, I. D. Boyd, Momentum and heat transfer in a laminar boundary layer with slip flow, Journal of thermophysics and heat transfer, 20(4) (2006) 710-719.
[5]. F. S. Ibrahim, A. M. Elaiw, A. A. Bakr, Effect of the chemical reaction and radiation absorption on the unsteady MHD free convection flow past a semi infinite vertical permeable moving plate with heat source and suction, Communications in Nonlinear Science and Numerical Simulation, 13(6) (2008) 1056-1066.

[6]. M. S. Abel, P. S. Datti, N. Mahesha, Flow and heat transfer in a power-law fluid over a stretching sheet with variable thermal conductivity and non-uniform heat source, International Journal of Heat and Mass Transfer, 52(11-12) (2009) 2902-2913.
[7]. A. A. Abdul, Similarity solution for laminar thermal boundary layer over a flat plate with a convective surface boundary condition, Communications in Nonlinear Science and Numerical Simulation, 14(4) (2009) 1064-1068.
[8]. Cao, Kang, and John Baker. Slip effects on mixed convective flow and heat transfer from a vertical plate, International Journal of Heat and Mass Transfer, 52(15-16) (2009) 3829-3841.
[9]. I. Anuar, R. Nazar, I. Pop, Heat transfer over an unsteady stretching permeable surface with prescribed wall temperature, Nonlinear Analysis: Real World Applications, 10(5) (2009) 2909-2913.
[10]. T. Fang, J. Zhang, S. Yao, Slip MHD viscous flow over a stretching sheet–an exact solution, Communications in Nonlinear Science and Numerical Simulation, 14(11) (2009) 3731-3737.
[11]. M. M. Rahman, M. Mohammad, A. Aziz, A. M. l-Lawatia, Heat transfer in micropolar fluid along an inclined permeable plate with variable fluid properties, International Journal of thermal sciences, 49(6) (2010) 993-1002.
[12]. T. Hayat, M. Qasim, S. Mesloub, MHD flow and heat transfer over permeable stretching sheet with slip conditions, International Journal for Numerical Methods in Fluids, 66(8) (2011) 963-975.
[13]. M. H. Yazdi, S. Abdullah, I. Hashim, K. B. Sopian, Slip MHD liquid flow and heat transfer over non-linear permeable stretching surface with chemical reaction, International Journal of Heat and Mass Transfer, 54(15-16) (2011) 3214-3225.
[14]. M. M. Rahman, Locally similar solutions for hydromagnetic and thermal slip flow boundary layers over a flat plate with variable fluid properties and convective surface boundary condition, Meccanica, 46(5) (2011) 1127-1143.
[15]. A. A. Mostafa Mahmoud, MHD flow and heat transfer in a viscous fluid over a non-isothermal stretching surface with thermal radiation in slip-flow regime, Chemical Engineering Communications, 199(7) (2012) 925-942.
[16]. S. Kunal, K. N. Premnath, Effect of magnetic field on the natural convection from a vertical melting substrate, International journal of thermal sciences, 53(2012) 89-99.
[17]. M. Turkyilmazoglu, Exact analytical solutions for heat and mass transfer of MHD slip flow in nanofluids, Chemical Engineering Science, 84(2012) 182-187.
[18]. O. D. Makinde, Effect of variable viscosity on thermal boundary layer over a permeable flat plate with radiation and a convective surface boundary condition, Journal of Mechanical Science and Technology, 26(5) (2012) 1615-1622.
[19]. I. Wubshet, B. Shankar, MHD boundary layer flow and heat transfer of a nanofluid past a permeable stretching sheet with velocity, thermal and solutal slip boundary conditions, Computers & Fluids, 75 (2013) 1-10.
[20]. K. Das, S. Jana, P. K. Kundu, Thermophoretic MHD slip flow over a permeable surface with variable fluid properties, Alexandria Engineering Journal, 54(1) (2015) 35-44.
[21]. S. K. Parida, S. Panda, B. R. Rout, MHD boundary layer slip flow and radiative nonlinear heat transfer over a flat plate with variable fluid properties and thermophoresis, Alexandria Engineering Journal, 54(4) (2015) 941-953.
[22]. J. C. Umavathi, A. J. Chamkha, S.Mohiuddin, Combined effect of variable viscosity and thermal conductivity on free convection flow of a viscous fluid in a vertical channel, International Journal of Numerical Methods for Heat & Fluid Flow, 26(1) (2016) 18-39.
[23]. M. M. Nandeppanavar, M. C. Kempraju, R. Madhusudhan, S. Vaishali, MHD slip flow and convective heat transfer due to a moving plate with effects of variable viscosity and thermal conductivity, Multidiscipline Modeling in Materials and Structures,16(5) (2020) 991-1018.

HIMANSHU CHAUDHARY[1*],DEENA SUNIL[2], VISHNU NARAYAN MISHRA[3]

Research Scholar, Department of mathematics, Indira Gandhi National Tribal University,Amarkantak, Madhya Pradesh, India

Assistant Professor, Department of mathematics, Indira Gandhi National Tribal University, Amarkantak, Madhya Pradesh, India

Professor, Department of mathematics, Indira Gandhi National Tribal University, Amarkantak, Madhya Pradesh, India

[1*]*himanshuigntu2020@gmail.com*, [2]*deena.sunil@igntu.ac.in*[3]*vishnunarayanmishra@gmail.com*